# GCOM–C1/SGLI Land Surface Temperature Product Algorithm Theoretical Basis Document

Masao Moriyama
Nagasaki University
Nagasaki, JAPAN.

Spt. 30, 2014

# Contents

# List of Figures

# List of Tables

# Chapter 1

# Introduction

This document describes the land surface temperature estimation algorithm for SGLI sensor. So far the land surface temperature estimation from space is made by many kinds of sensors, as the operational product, ASTER and MODIS onboard TERRA satellite made the land surface temperature product in late 90's. Just after this, ATS oboard the European satellite ESA published the land surface product. The operational land surface temperature estimation has about 10 years history and the improvement of the estimation algorithm are made.

For SGLI, the land surface temperature estimation algorithm will be made on the basis of these previous algorithm and will be added the new improvement. The split window algorithm is used for MODIS and AATSR, this is less computation time and suitable for the wide swath sensor but the surface emissivity has to be the known variable. On the other hand, ASTER uses the semi–analytical method to estimate not only the surface temperature but the emissivity, but it's computation time consumable. For SGLI, the semi–analytical method which uses the split window algorithm as the constraint of the land surface temperature/emissivity and the observed brightness temperature.

From the next chapter, the split windows algorithm, the semi–analytical algorithm will be described. And also the operational factor such as input and output and the data processing flow will be explained. At the end of this document, the validation plan will be noticed.

# Chapter 2

# Split window algorithm

## 2.1 Physics of the LST estimation algorithm

The satellite detected radiance at $i$ th. observation channel $I_i$ is described as the following radiative transfer equation.

$$I_i = \tau_i(\theta) I_{si} + I_{ai}(\theta) \tag{2.1}$$

where $\tau$, $\theta$, $I_s$ and $I_a$ are the total transmittance, the observation zenith, the land leaving radiance and the path radiance respectively. And the land leaving radiance is expressed as Eq. (2.2).

$$I_{si} = \varepsilon_i B_i(T_s) + (1 - \varepsilon_i)\frac{F_i}{\pi} \tag{2.2}$$

where $\varepsilon$, $B$, $T_s$ and $F$ are the surface emissivity, Planck function, the surface temperature and the downward atmospheric irradiance respectively. Even the atmospheric condition is known, the land leaving radiance contains two kinds of unknowns, surface temperature and emissivity. Since the surface emissivity has the spectral dependency, this problem is underdetermine in any numbers of the observation spectral channels.

## 2.2 Overview of the split window algorithm

Since the sea surface can be assumed the blackbody and the temperature range is up to 30 [K], The difference between the sea surface temperature (SST) and the satellite detected brightness temperature is caused by the atmospheric effect. Deschamps *et al.* found that the brightness temperature difference of 10.8 and 12.0 [$\mu$m] spectrum over the sea surface contains the atmospheric effect and found the linear relationship between the difference of the true SST and the 10.8 [$\mu$m] spectrum brightness temperature [Deschamps and Phulpin, 1980]. After some improvements, the multiple regression formula between the brightness temperature of 10.8 and 12.0 [$\mu$m] spectrum and the sea surface temperature which is called Multiple Channel Sea Surface Temperature estimation scheme (MCSST) [McClain et al., 1985] is established for the satellite based SST estimation. The MCSST formula is shown in Eq. (2.3),

$$T_s = C_0 + C_1 T_1 + C_2(T_1 - T_2) \tag{2.3}$$

where $T_s$, $T_1$, $T_2$ and $C$s are sea surface temperature, brightness temperature at 10.8 and 12.0 [$\mu$m] spectrum and the regression coefficients respectively. The MCSST formula is widely used for about 40 years and continues to make the high accuracy SST estimation. So that the SGLI land surface temperature (LST) estimation algorithm starts from the MCSST formula and this is modified for the LST estimation.

## 2.3 Difference from SST estimation and modification

There are many types of the covering category of the land, although that of the sea is only one, water. This variety of the land cover makes the temperature estimation difficult. The differences between the LST and SST estimation from the satellite are the followings.

1. The dynamic range of LST is wider than that of SST.
2. The land surface emissivity varies considerably, hence the sea surface emissivity is almost constant.

To compensate these 2 difference, the following modification are made.

### 2.3.1 Dynamic range compensation

For the sea surface case, the evaporation suppress the temperature increase so that the SST is almost same as the surface air temperature, but the land surface case, especially the dry area in the daytime, the evaporation cannot be expected so that the surface temperature is so much larger than the surface air temperature. As an example of this, the surface air temperature and the surface temperature on 18:00(GMT), 1 July 2005 extracted from the NCEP reanalysis data are shown in Figure 2.1. Around the great basin area, the difference between the surface temperature and the surface air temperature is more than 10[K].

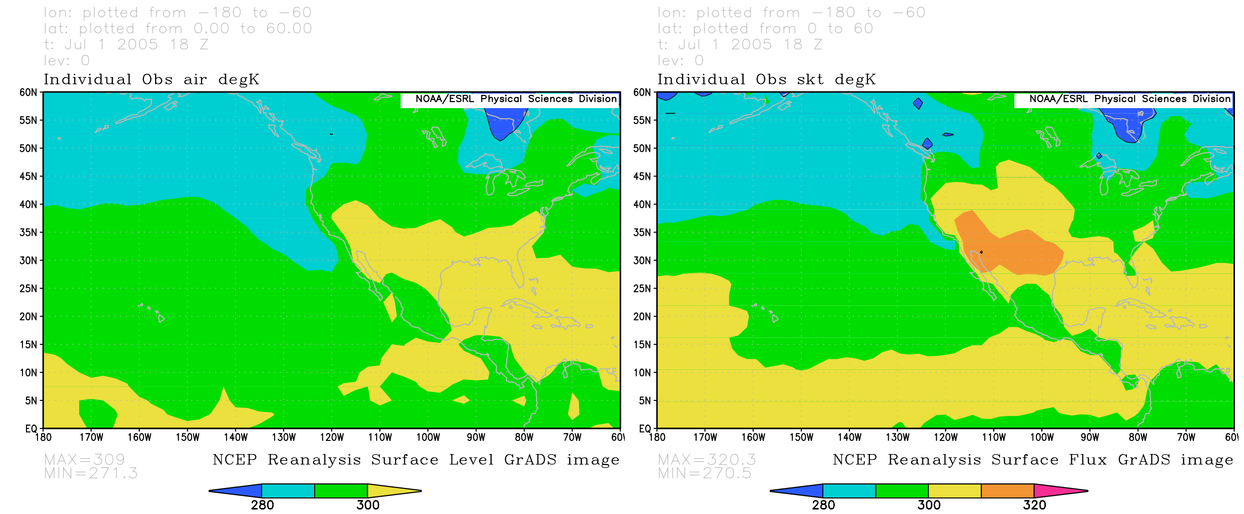


Figure 2.1: The surface air temperature (Left) and the surface temperature (Right) on 18:00, 1 July 2005.

To confirm the MCSST formula works in the case of the wide surface temperature range, the numerical simulation is made that the satellite detected brightness temperature is computed under the condition shown in Table 2.1 using MODTRAN and define the regression coefficients in MCSST formula. The RMS difference between the model and estimated surface temperature is enough small (0.53[K]), so that the MCSST formula can compensate the wide surface temperature range in the case of the blackbody surface. The relationship between the 2 kinds of the temperature difference is shown in Figure 2.3.

Table 2.1: The surface temperature range simulation condition

| | |
|---|---|
| Atmospheric profile | Longitudinal mean with $10^o$ latitude interval of 2000 ECMWF monthly mean atmosphere |
| Surface emissivity | 1.0 |
| Surface temperature | Surface air temperature + 0, 5, 10, 15 [K] |
| Observation zenith | 0, 15, 30, $45^o$ |
| Target sensor | MODIS chs. 31, 32 (*cf.* Figure 2.2) |

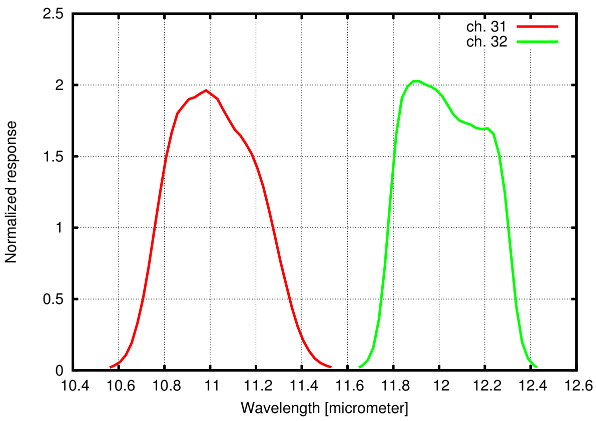


Figure 2.2: MODIS chs. 31, 32 normalized response.

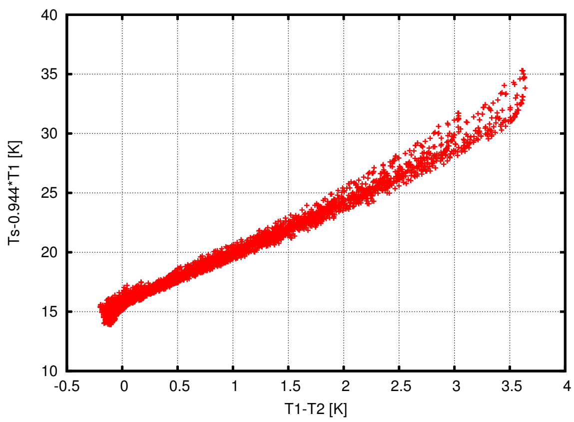


Figure 2.3: Relationship of the 2 kinds of the temperature difference

As a result, the linear relationship can be established as Eq(2.4) for the wide surface temperature range blackbody observed case.

$$T_s = C_0' + C_1' T_1' + C_2'(T_1 - T_2') \tag{2.4}$$

where $T_1'$, $'_2$ ans $C'$ are the blackbody observed brightness temperature at 10.8 and 12.0 [$\mu$m] spectrum and the regression coefficients respectively.

### 2.3.2 Surface emissivity compensation

Same as the current similar sensor such as AATSR and MODIS, SGLI LST estimation algorithm treat the surface emissivity as the known variables [Prata, 2002, Wan, 1999]. Since the MCSST formula works over the blackbody surface in the case of the wide surface temperature range, if the blackbody surface observed brightness temperature is estimated from the actual non–blackbody surface observed brightness temperature, the MCSST formula can estimates LST under the non–blackbody surface [Moriyama, 2009]. The above assumption is verified through the following numerical simulation.

The various land cover materials' emissivity is summarized as the spectral library [Salisbery and D'Aria, 1985]. From the spectral library, the spectral emissivity of MODIS chs. 31, 32 are computed and shown in Figure 2.4. The emissivity category as shown in Figure 2.5 and compute the satellite detected brightness temperature under the condition in Table 2.2. The comparison between the blackbody and non–blackbody observed brightness temperature at MODIS chs. 31, 32 are made.

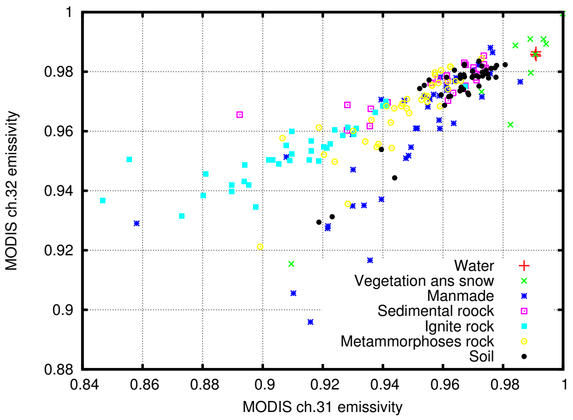


Figure 2.4: Various materials' emissivity

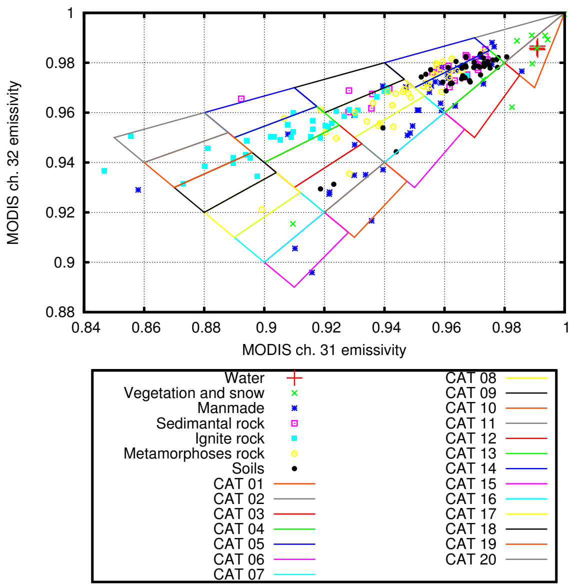


Figure 2.5: Emissivity categories

Table 2.2: The surface temperature range simulation condition

| | |
|---|---|
| Atmospheric profile | Longitudinal mean with $10^o$ latitude interval of 2000 ECMWF monthly mean atmosphere |
| Surface emissivity | 1.0, Average of each emissivity category |
| Surface temperature | Surface air temperature + 0, 5, 10, 15 [K] |
| Observation zenith | 0, 15, 30, $45^o$ |
| Target sensor | MODIS chs. 31, 32 (*cf.* Figure 2.2) |

The comparison results are shown in Figure 2.6. From the results, the linear relationship is found, so that the following conversion formula from the non-blackbody observed brightness temperature $T_i$ to the blackbody observed brightness temperature $T_i'$.

$$T_i' = a_i T_i + b_i \tag{2.5}$$

where subscript $i$, $a$ and $b$ are spectral channel and constants respectively. At each emissivity category, the coefficients are defined by the least square method. The coefficients and RMS error are shown in Table 2.3.

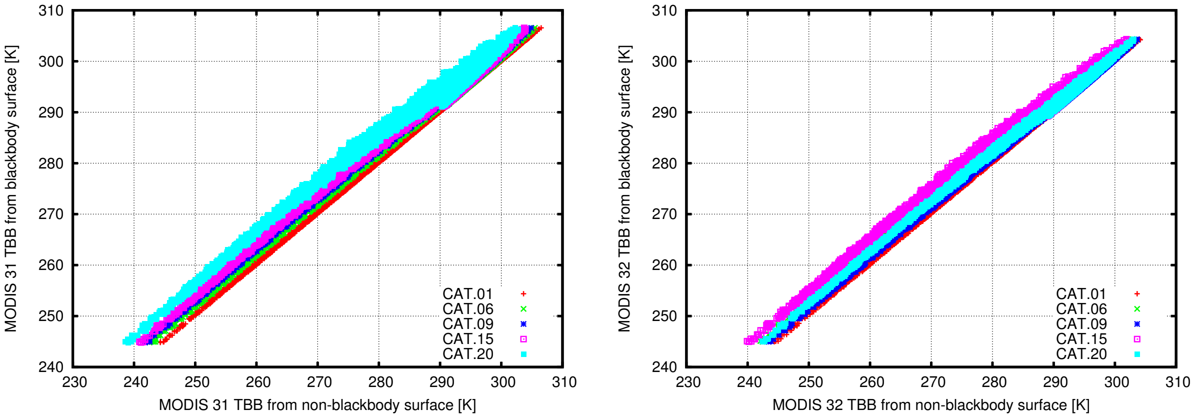


Figure 2.6: Comparison between blackbody and non–blackbody observed brightness temperature at MODIS ch. 31 (Left) and 32 (Right)

Table 2.3: Regression coefficients and RMS error of the blackbody observed brightness temperature estimation

| | MODIS ch. 31 | | | MODIS ch. 32 | | | Emissivity | |
|---|---|---|---|---|---|---|---|---|
| CAT. | $a$ | $b$ | RMS[K] | $a$ | $b$ | RMS[K] | MODIS ch. 31 | MODIS ch. 32 |
| 01 | 0.995 | 1.748 | 0.196 | 0.988 | 3.869 | 0.317 | 0.992 | 0.987 |
| 02 | 0.991 | 2.900 | 0.316 | 0.993 | 2.261 | 0.196 | 0.988 | 0.993 |
| 03 | 0.982 | 6.002 | 0.354 | 0.968 | 10.238 | 0.476 | 0.974 | 0.966 |
| 04 | 0.977 | 7.735 | 0.452 | 0.975 | 7.977 | 0.375 | 0.966 | 0.974 |
| 05 | 0.971 | 9.584 | 0.547 | 0.982 | 5.756 | 0.275 | 0.959 | 0.981 |
| 06 | 0.969 | 10.558 | 0.542 | 0.948 | 16.565 | 0.681 | 0.954 | 0.946 |
| 07 | 0.963 | 12.503 | 0.634 | 0.956 | 13.974 | 0.580 | 0.946 | 0.954 |
| 08 | 0.957 | 14.454 | 0.727 | 0.964 | 11.435 | 0.482 | 0.938 | 0.962 |
| 09 | 0.951 | 16.444 | 0.822 | 0.972 | 8.870 | 0.381 | 0.929 | 0.971 |
| 10 | 0.955 | 15.152 | 0.735 | 0.929 | 22.622 | 0.895 | 0.934 | 0.926 |
| 11 | 0.948 | 17.280 | 0.829 | 0.937 | 19.941 | 0.797 | 0.926 | 0.934 |
| 12 | 0.942 | 19.351 | 0.920 | 0.946 | 17.253 | 0.696 | 0.917 | 0.943 |
| 13 | 0.936 | 21.436 | 1.011 | 0.954 | 14.550 | 0.595 | 0.908 | 0.952 |
| 14 | 0.929 | 23.524 | 1.103 | 0.963 | 11.871 | 0.494 | 0.900 | 0.961 |
| 15 | 0.940 | 19.902 | 0.929 | 0.910 | 28.537 | 1.106 | 0.914 | 0.905 |
| 16 | 0.934 | 22.101 | 1.019 | 0.918 | 25.838 | 1.007 | 0.905 | 0.914 |
| 17 | 0.927 | 24.262 | 1.111 | 0.927 | 23.116 | 0.907 | 0.896 | 0.923 |
| 18 | 0.921 | 26.435 | 1.202 | 0.936 | 20.357 | 0.807 | 0.888 | 0.933 |
| 19 | 0.914 | 28.588 | 1.294 | 0.945 | 17.643 | 0.705 | 0.879 | 0.942 |
| 20 | 0.907 | 30.833 | 1.385 | 0.953 | 14.915 | 0.604 | 0.869 | 0.951 |

By comparing the coefficients and the emissivity, the linear relationship between the surface reflectivity ($r_i = 1-\varepsilon_i$) and the coefficients can be found as Figure 2.7. From the results, the blackbody observed brightness temperature estimation formula is express as the function of surface reflectivity and the non–blackbody observed brightness temperature as Eq. (2.6).

$$T_i' = (a_i r_i + b_i)T_i + (c_i r_i + d_i) \tag{2.6}$$

where $a$, $b$, $c$, $d$ are the constants. From Eqs. (2.4, 2.6), the following SGLI split window LST estimation algorithm is established.

$$T_s = A_0 + (A_1 r_1 + A_2)T_1 + A_3 r_1 + (A_4 r_2 + A_5)T_2 + A_6 r_2 \tag{2.7}$$

where $A$s are the regression coefficients. This formula is used for the standard algorithm of the GCOM–C1/SGLI LST product.

From the condition in Table 2.2, The regression coefficients of Eq. (eq:sglilst) are defined by the least square method and compute the RMS error of the estimated LST, From the same condition, the regression coefficients of the MODIS Generalized Split Window algorithm (GSW) [Wan, 1999] as Eq. (2.8) are also defined and compute the RMS error.

$$Ts = \left( A_1 + A_2 \frac{1-\bar{\varepsilon}}{\bar{\varepsilon}} + A_3 \frac{\Delta\varepsilon}{\bar{\varepsilon}^2} \right) \frac{T_1 + T_2}{2} + \left( B_1 + B_2 \frac{1-\bar{\varepsilon}}{\bar{\varepsilon}} + B_3 \frac{\Delta\varepsilon}{\bar{\varepsilon}^2} \right) \frac{T_1 - T_2}{2} + C \tag{2.8}$$

where $A$, $B$, $C$ are the regression coefficients and $\bar{\varepsilon}$ and $\Delta\varepsilon$ are the average and difference of the surface emissivity at the 10.8 and 12.0 [$\mu$m] spectrum respectively.

The RMS error in the case of the SGLI split window is 1.46[K] hence that in the case of MODIS GSW is 1.50[K]. The comparison between the model and estimated LST in the case of SGLI split window and MODIS GSW are shown in Figure 2.8. The SGLI split window algorithm has the comparable accuracy with the MODIS GSW algorithm.

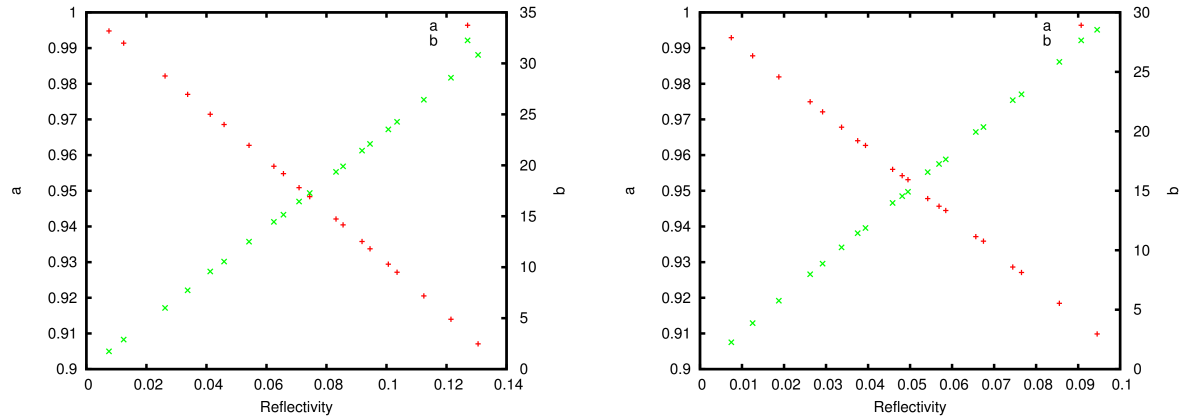


Figure 2.7: Relationship between blackbody observed brightness temperature conversion coefficients and the surface reflectivity at MODIS ch. 31 (Left) and 32 (Right)

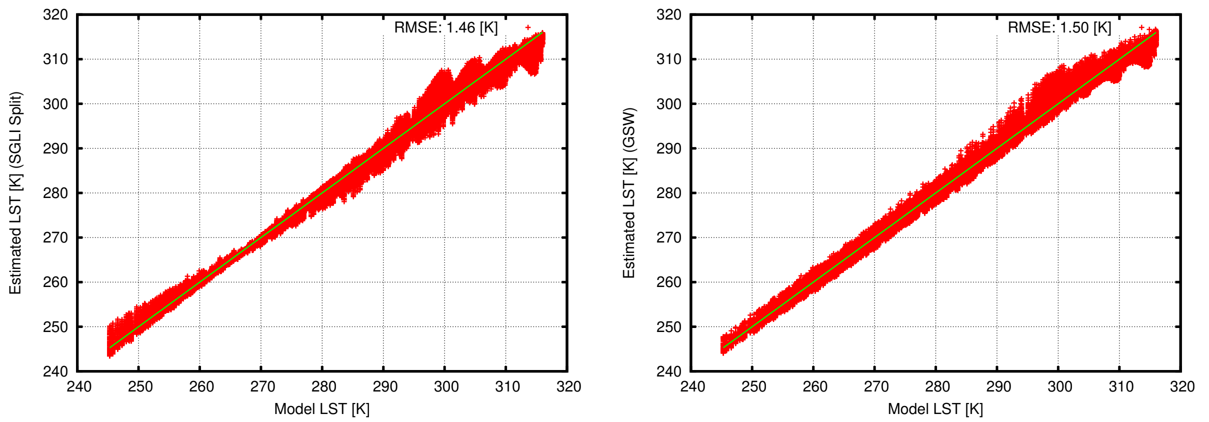


Figure 2.8: Comparison between the model and estimated LST in the case of SGLI (Left) and MODIS (Right)

## 2.4 Accuracy and stability

### 2.4.1 Effect of the assumptions of the blackbody observed brightness temperature estimation

The RMS error of the MCSST formula in the case of the blackbody observation as Eq. (2.4) is about 0.53[K], on the other hand the RMS error of the blackbody observed brightness temperature estimation as Eq. (2.5) is up to about 1.4[K] as shown in Table 2.3. So this assumption error is considered as one of the most significant LST estimation error causes. This assumption error assumed to be caused by the wide range of the surface temperature because of the non–linearity of the Planck function. To estimate the surface temperature range effect to the assumption error, the numerical simulation almost same as the previous blackbody observed brightness temperature estimation except the surface temperature range. In this case the surface temperature range is limited to the same as 5[K] above the surface air temperature, ans the other conditions are the same as Table 2.2. The comparison between RMS error of the blackbody observed brightness temperature under the all cases and low cased of the surface temperature is made and shown in Figure 2.9. The result shows that the blackbody observed brightness temperature estimation is accurate under the low surface temperature case.

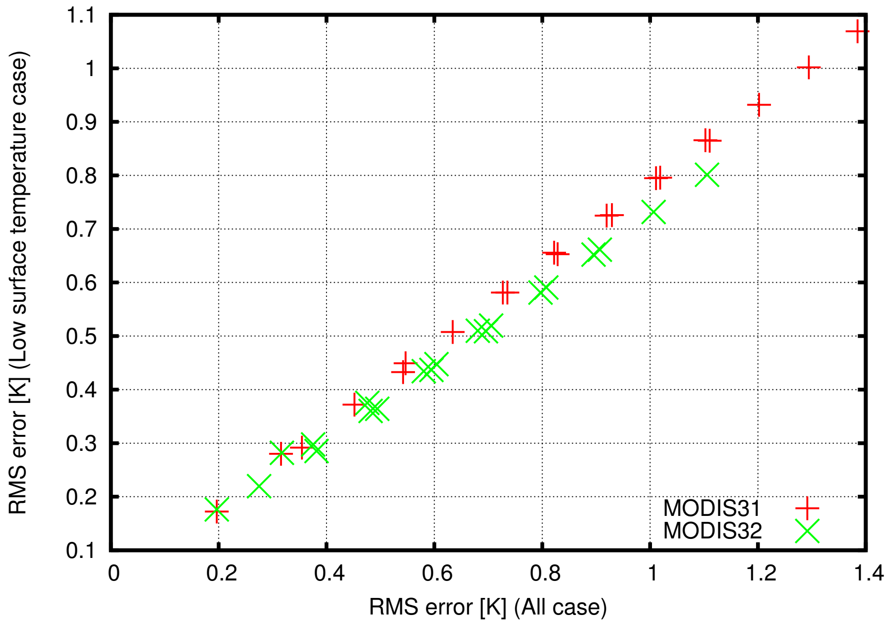


Figure 2.9: Comparison between the RMS error of the blackbody observed brightness temperature estimation under the all and low surface temperature cases

To reduce the LST estimation error, 2 sets of the regression coefficients set will be defined for the high and low surface temperature cases. The coefficient set selection scheme will be the daytime/nighttime determination because in the nighttime, the surface temperature of almost all land cover category will be balanced to the surface air temperature.

### 2.4.2 Emissivity misestimation effect

Since all measurement contain the observation error, the algorithm developer must consider the error propagation to the final product. Generally, the error propagation theory [Tayler, 1997] is used for the purpose as Eq. (2.9).

$$\begin{aligned} y &= f(x_1, x_2, \ldots, x_n) \\ \delta y &= \sum_{i=1}^{n} \frac{\partial y}{\partial x_i} \delta x_i \end{aligned} \tag{2.9}$$

where $y$, $x$, $f$ and $\delta$ are the output variable, input variables, the function from the input to the output and the suffix means small change of the variable respectively.

The alternate cause of the LST estimation error using split window algorithm is the misestimation of the surface emissivity. To estimate the emissivity misestimation effect, Eq. (2.9) is used with the variable conversion of $x_i = \varepsilon_i$ and $y = T_s$. The estimated surface temperature change relevant to 0.01 overestimated surface emissivity under the condition in Table 2.2 are computed in the case of SGLI split window algorithm and MODIS GSW algorithm. The results are shown in Figure 2.10.

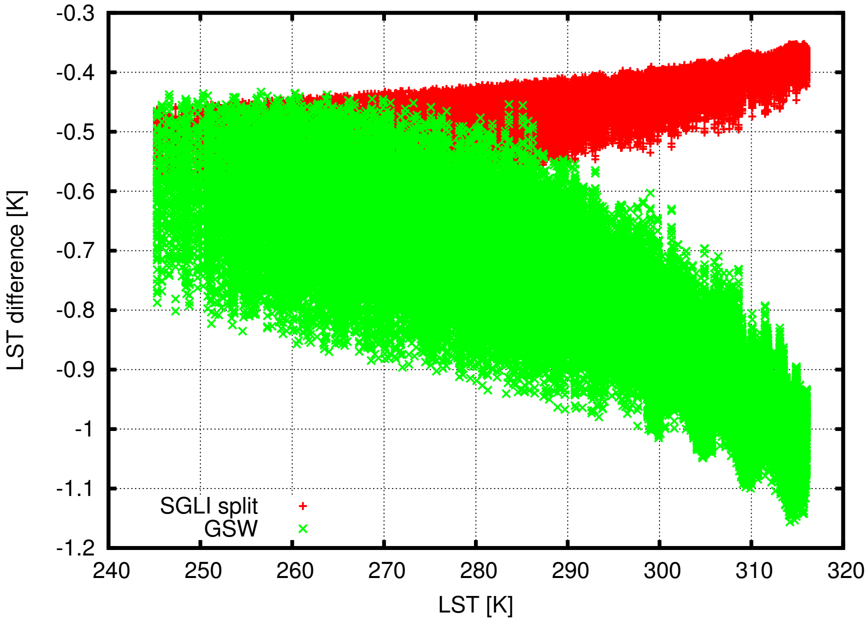


Figure 2.10: LST difference relevant to 0.01 overestimated surface emissivity

The results show that the estimated LST difference relevant to the misestimated surface emissivity in the case of SGLI split window algorithm is almost smaller than that in the case of MODIS GSW algorithm. This means that SGLI split window algorithm is more insensible with the misestimated surface emissivity than MODIS GSW algorithm. This fact will be the big advantage of SGLI split window algorithm.

# Chapter 3

# Semi–analytical LST estimaton algorithm

## 3.1 Overview

As explained before, the land leaving radiance (*cf.* Eq. (2.2)) has two unknowns, the surface temperature and emissivity, and the surface emissivity has spectral dependency. Since this problem becomes underdetermine, reduction of the unknown or addition of the extra formula is necessary to solve this problem. ASTER LST estimation algorithm uses the additional formula which is defined from the statistics of the spectral emissivity of the 5 TIR observation channels. But for the less observation channel sensor such as AVHRR, MODIS, there were no additional formula because the two observation channels are not enough to establish the spectral emissivity relationship.

### 3.1.1 Integration of the split window method and semi–analytical method

From the other viewpoint, the SGLI LST split window formula is regarded as the statistical relationship between the observed value and the unknown variables and it has the enough accuracy so that this formula can be the additional formula to the semi–analytical method. In this case, since the split window method contains the satellite detected brightness temperature, the following simultaneous equation (Eq. (3.1 – 3.3)) which contains the radiative transfer equation which expresses the satellite detected brightness temperature instead of the land leaving radiance.

$$T_1 = B_1^{-1}[\tau_1(\varepsilon_1 B_1(T_s) + (1-\varepsilon_1)\frac{F_1}{\pi}) + I_{a1}] \tag{3.1}$$

$$T_2 = B_2^{-1}[\tau_2(\varepsilon_2 B_2(T_s) + (1-\varepsilon_2)\frac{F_2}{\pi}) + I_{a2}] \tag{3.2}$$

$$T_s = (A_1 + A_2 r_1)T_1 + A_3 r_1 + (A_4 + A_5 r_2)T_2 + A_6 r_2 + A_0 \;\; (r_i = 1-\varepsilon_i) \tag{3.3}$$

where $B^{-1}$ is the Inverse Planck function. Among this simultaneous equation, the brightness temperature $T_1$ and $T_2$ are the observed value, the transmittance $\tau$, the path radiance $I_a$ and the downward atmospheric irradiance $F$ is the computed value from the atmospheric condition and the surface temperature $T_s$ and the emissivity $\varepsilon$ are the solutions. To solve this simultaneous equation, the Newtonian iteration scheme is used.

## 3.2 Validation

### 3.2.1 Numerical simulation for the accuracy verification

For the accuracy verification, the LST estimation using the numerical simulated observed radiance is made. The simulation condition is listed in Table 3.1, in the table, the average emissivity $\bar{\varepsilon}$ and the spectral dependency parameter $a$ are defined as follows.

$$\bar{\varepsilon} = \frac{\varepsilon_1 + \varepsilon_2}{2}, \quad \delta\varepsilon = \frac{\varepsilon_1 - \varepsilon_2}{2}, \quad a = \frac{\delta\varepsilon}{1-\bar{\varepsilon}}, \quad (-1 < a < 1) \tag{3.4}$$

$$\varepsilon_1 = \bar{\varepsilon} + (1-\bar{\varepsilon})a, \quad \varepsilon_2 = \bar{\varepsilon} - (1-\bar{\varepsilon})a \tag{3.5}$$

Table 3.1: The semi–analytical method simulation condition

| Atmospheric profile | Longitudinal mean with $10^o$ latitude interval of 2000 ECMWF monthly mean atmosphere |
|---|---|
| $\bar{\varepsilon}$ | 0.94, 0.95, 0.96, 0.97, 0.98, 0.99 |
| $a$ | -0.5, -0.25, 0, 0.25, 0.5 |
| Surface temperature | Surface air temperature + 0, 5, 10, 15 [K] |
| Observation zenith | 0, 15, 30, $45^o$ |
| Observation error | 0.2 [K] (@300 [K]) |
| Max. iteration | 10 |

As the results, RMS residual of the simultaneous equation histogram, LST estimation error and the emissivity estimatation error are shown in Figure 3.1. The results show the estimation accuracy closely depends on the RMS residual between the both hand side of the simultaneous equation Eq. (3.1–3.3), In the case of the RMS residual is less than 1 [K], LST estimation error is less than 1.5 [K], almost same as the case of the split window method even the surface emissivity is unknown.

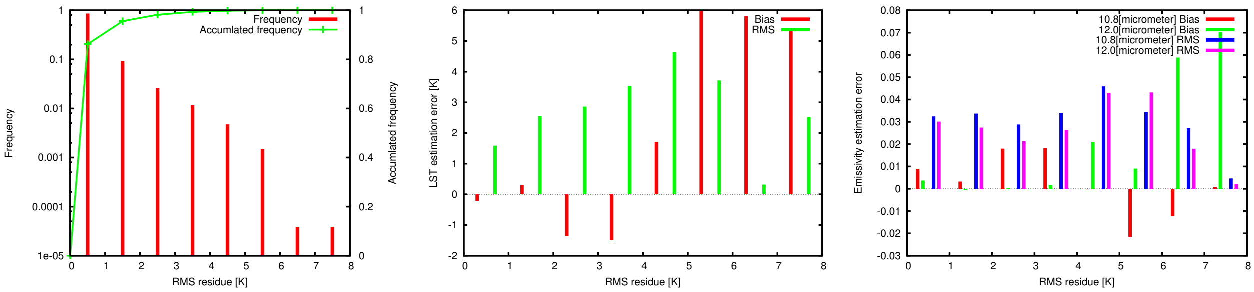


Figure 3.1: The numerical simulation results Left: RMS residue histogram, Middle: LST estimation error, Right: Emissivity estimation error

### 3.2.2 Cross Validation

**Outline**

Since the surface temperature varies temporally and spatially, the LST ground truth dataset is difficult to gather. So in this paper, the cross validation between the proposed method and the other LST product. As the comparison, MODIS daily global mapped Day/Night land surface temperature and emissivity product (MOD11C1) is used [Wan, 1999]. This product is made by the Day/Night algorithm which solve the simultaneous radiative transfer equation of the day and night observed radiance of 6 emission spectral channel data at the same location. The surface emissivity is from the land cover classification data as an input and the day and night surface temperature are the solution of this algorithm. If surface temperature and emissivity satisfy the radiative transfer equation, these are marked as "GOOD" in the product quality assurance (QA) field. Moreover, the Day/Night algorithm has the least assumptions in the present time. Figure 3.2 show the daytime LST and Daytime GOOD pixel on Dec. 31 2009.

**Validation Scheme**

MODIS Day/Night LST product compensates the misalignment of the pixel with the spatial averaging into 5 × 5 pixel and MOD11C1 product reaveraged into the global 0.05 [deg.] grid. In this study, the input of

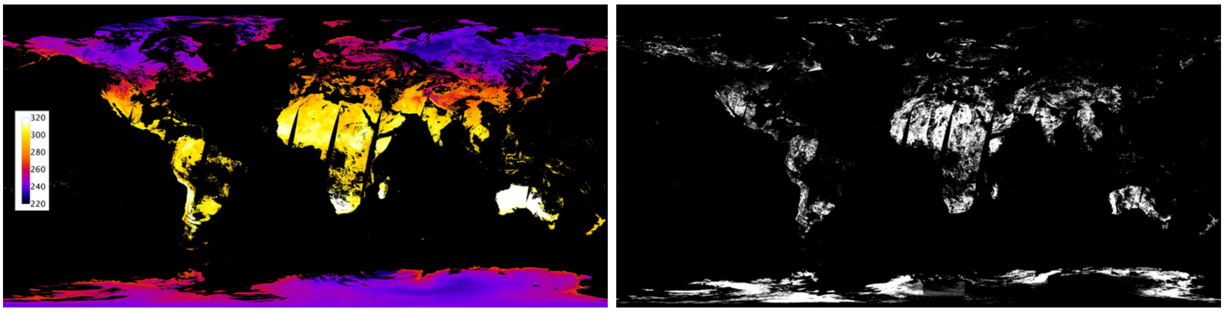


Figure 3.2: Dec. 31 2009 MOD11C1 product, Left: Daytime LST, Right: Daytime GOOD pixel (white)

the semi–analytical LST estimation method is TERRA/MODIS 1 [km] resolution Satellite detected radiance (MOD02) acquired at 1835Z and 0400Z of every day in 2000, the estimated temperature and emissivity are averaged into 0.05 [deg.] grid and are compared with MOD11C1 product. As the auxiliary data, the MODIS location information (MOD03), the MODIS cloud mask (MOD35) and the nearest time NCEP 1 [deg.] mesh forecasting data are used. As an example of the semi–analytical method output, the true color composite, the estimated LST and emissivity of TERRA/MODIS data which acquired on 0400Z Spt. 15 2000 are shown in Figure 3.3.

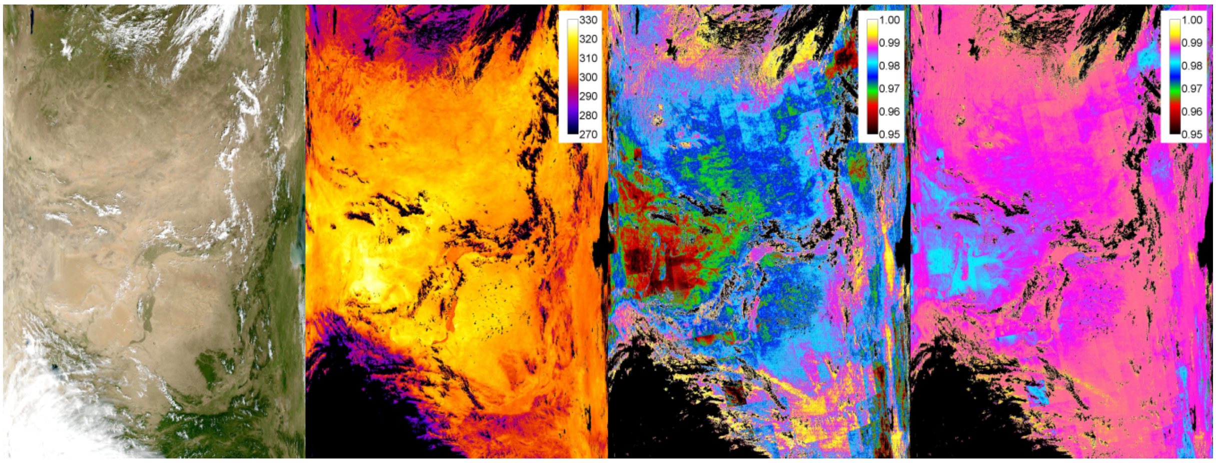


Figure 3.3: LST and emissivity estimation result from TERRA/MODIS data aquired on 0400Z Spt. 15 2000 (from Left to Right: True color composite, LST, emissivity at ch. 31, emissivity at ch. 32)

### LST comparison result

The scene center of each 1835Z and 0400Z MOD02 data are shown in Figure 3.4 and the bias and RMS difference between the MOD11C1 LST and averaged LST from semi–analytical method are shown in Figure 3.5.

In the case of many averaged pixel, the bias and RMS difference is small, in other words, the less cloud scene shows the good correspondence between two kinds of estimated LST. To clarify the cloud effect, the comparison between two kind of estimated LST with the different averaged pixel number within the 0.05 [deg.] grid in Figure 3.6 and 3.7. The large number of the averaged pixel mea ns this pixel is clear, so the proposed method shows the good correspondence with the MODIS Day/Night LST product.

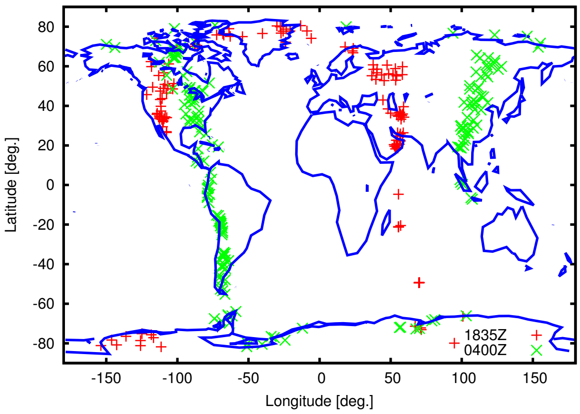

Figure 3.4: The scene center of MOD02 data

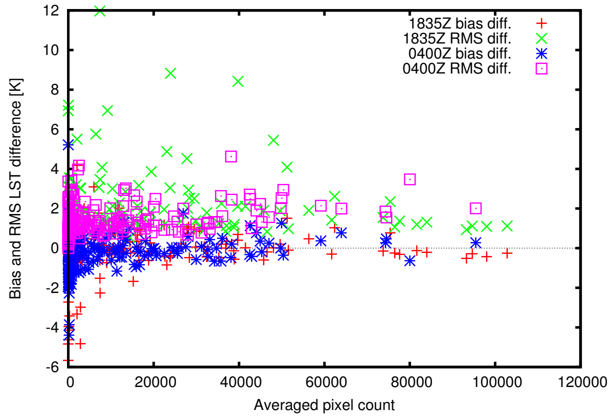

Figure 3.5: LST estimation error

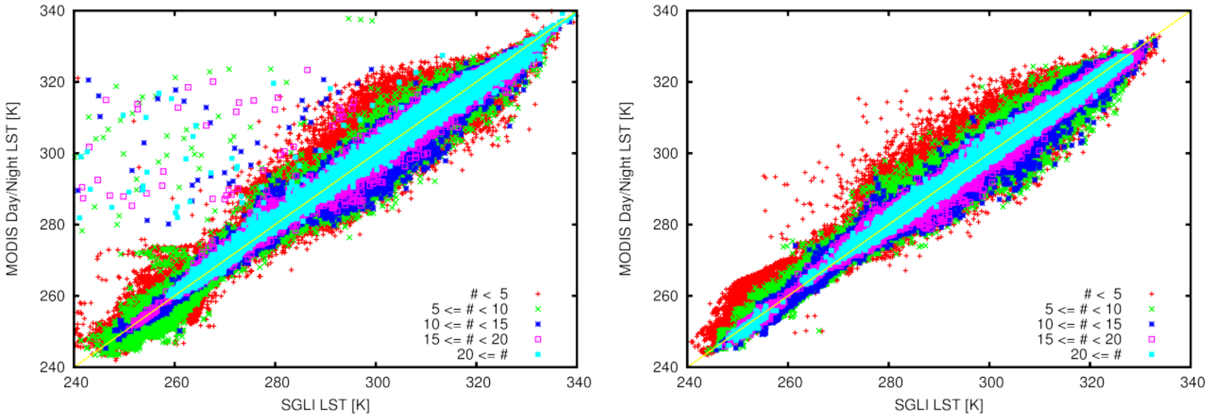

Figure 3.6: Comparison between two kinds of LST (Left: 1835Z, Right: 0400Z)

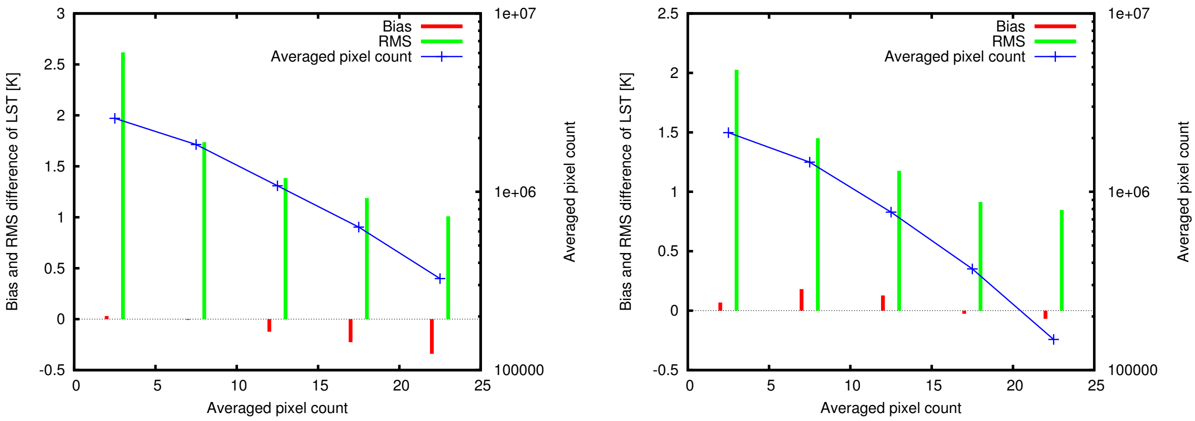

Figure 3.7: LST difference histogram (Left: 1835Z, Right: 0400Z)

## 3.3 Quality assurance

### 3.3.1 Concept

To notice the users about the quality of the product as well as the selection key of the spatial/temporal integration, the quality assurance (QA) field is necessary. The structure of the QA field of the previous remote sensing data products have their own style. For example, MODIS and LANDSAT 8 show not only the quality but the quality check routine is applied or not. For SGLI/LST case the limitation of the data size, only the quality will be shown. The basic concept of the SGLI/LST QA field is “smaller value is better”, the value of zero of QA field is the best quality and the larget value of QA field means worse.

### 3.3.2 QA field bit assignment

SGLI/LST QA field has the single byte length and the bit assignment is shown in Table 3.2. If the bit 4 –7 is 1, the LST and emissivity set to 0. The residual of bit 1 and 2 is the RMS residual between the both hand side of the simultaneous equation Eq. (3.1–3.3). From the numarical simulation result (*cf.* Figure 3.1), the large residual (bit 2 is 1) means the residual is larget than 2[K], the fairly large residual (bit 1 is 1) means the residual is in the range of 1 to 2[K].

Table 3.2: SGLI/LST QA field (Bit 0 means LSB)

| Bit | Description |
|---|---|
| 7 | Non–data (=1) |
| 6 | Non–land (=1) |
| 5 | LST is out of range (=1) |
| 4 | Cloudy (=1) |
| 3 | Probably clear (=1) |
| 2 | Large residual (=1) |
| 1 | Fairly large residual (=1) |
| 0 | Transmittance of 11[$\mu$m] is below 0.6 (=1) |

# Chapter 4

# Operation

## 4.1 Input/Output dataset

The input dataset for LST estimation algorithm are summarized in Table 4.1. The output dataset are

Table 4.1: The input dataset

| | Dataset |
|---|---|
| a | Precise geometrically corrected radiance (250[m]) |
| b | Pixel wise Latitude and Longitude |
| c | Pixel wise scan zenith angle |
| d | Cloud flag |
| e | Land mask |
| f | Nearest time forecasting data (pressure, height, temperature, humidity) |

summarized in Table 4.2. These are stored in product HDF file as an independent plane.

Table 4.2: The output dataset

| | Dataset |
|---|---|
| A | Land surface temperature |
| B | Land surface temperature at 10.8 [$\mu$m] |
| C | Land surface temperature at 12.0 [$\mu$m] |
| D | QA files |

## 4.2 Data processing flow

The operation mode data processing flow are summarized in Figure 4.1. The precessing time for the single MODIS scene (Figure 3.3) with JMA forecasting dataset is about 25[sec.]

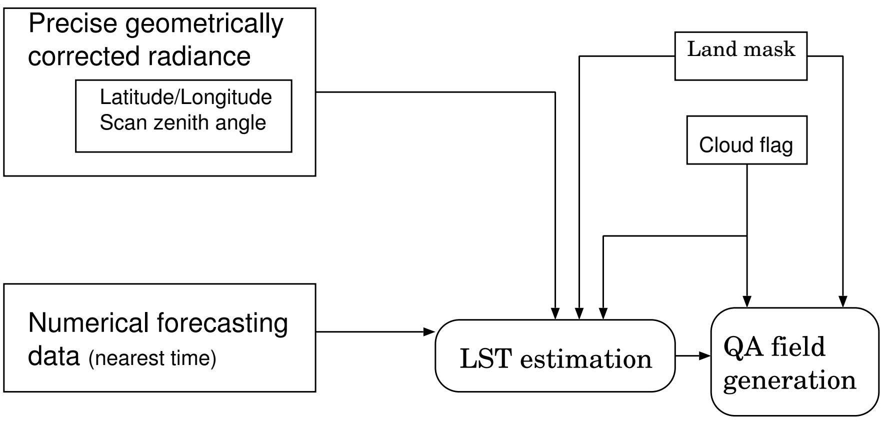


Figure 4.1: The data processing flow

# Chapter 5

# Validation

## 5.1 Basic concept of the validation of SGLI LST algorithm

Since the SGLI LST estimation algorithm contains the 2 kinds of algorithm, the split window algorithm for LST estimation and surface emissivity algorithm, the 2 kinds of validation will be made. The first one is the estimated LST validation and the second one is the estimated surface emissivity validation. Not only the following 2 kinds of validation, the cross comparison with the other satellite dataset such as NPP and SENTINEL will be made. Also the higher level products which use the LST product will be the validation factor which shows how does the LST product make the higher level products more accurate.

## 5.2 Estimated LST validation

SGLI LST estimation algorithm constructed under the 2 kinds of assumptions, MCSSTT formula can be applicable for the wide range of the blackbody surface temperature and the linear relationship can be established between the blackbody and non–blackbody observed brightness temperature. In the case that the surface emissivity is small, the second assumption (*cf.* Eq. (2.5)) is not so accurate by comparing with the accuracy of MCSST formula (*cf.* Eq. (2.4)).

The MCSST formula validation for the wide blackbody surface temperature range cannot be made in the natural condition because the blackbody or near blackbody surface temperature cannot be higher. For this purpose, the numerical simulation with the truth of the sea surface temperature and the calibration result.

For the estimated surface temperature validation in the low emissivity case, the ground measurement method of the surface temperature is established [Moriyama and Yano, 2000]. This method is for the bare soil area, using the wide FOV thermometer [Murayama and Moriyama, 1999] with the concave mirror the actual surface temperature can be measured without the emissivity measurement [Moriyama, 1999]. This data will be used for the validation. This kind of ground measurement will be made with the constant period, and using the ground measurement data and the numerically validated MCSST formula the total LST estimation algorithm will be validated in the case of the lower surface emissivity surface. This will be the worst case of the SGLI LST estimation. For the low emissivity case validation, the ground based LST observation synchronous with the TERRA and AQUA are made from 2000 to 2012 at Railroad valley playa, NV. USA. the comparison between the ground measured and estimted LST is shown in Figure 5.1. The total number of the data is 36 and the bias and RMS difference is 0.6[K] and 2.1[K].

## 5.3 Estimated emissivity validation

As the estimated surface emissivity validation, the semi–analytical surface emissivity estimation mode will be made and gather the surface emissivity data with the surface reflectance, the reflectance based surface emissivity formula will be more accurate. Also as the surface emissivity dataset, ASTER surface emissivity product and the FTIR sensor derived emissivity [Matsui and Moriyama, 2008] will be used for this purposes.

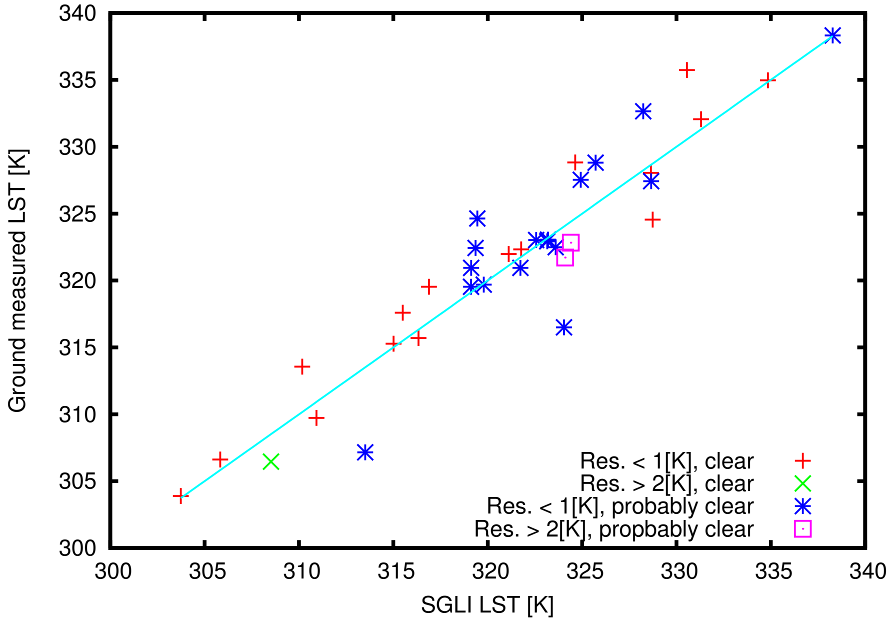


Figure 5.1: Comparison between the ground measured and the satellite derived LST

# Bibliography


[Deschamps and Phulpin, 1980] Deschamps, P. Y. and Phulpin, T., 1980. Atmospheric correction of infrared measurements of sea surface temperature using channels 3.7, 11 ans 12 $\mu$m. Boundary–Layer Meteor. 18, pp. 131–143.

[Matsui and Moriyama, 2008] Matsui, T. and Moriyama, M., 2008. Simultaneous estimation method of the surface temperature and emissivity from satellite based hyperspectral tir sensor. J. Remote Sens. of Japan 28(5), pp. 441–448.

[McClain et al., 1985] McClain, E. P., Pichel, W. G. and Walton, C. C., 1985. Comparative performance of avhrr–based multichannel sea surface temperature. J. Geophys. Res. 90, pp. 11587–11601.

[Moriyama, 1999] Moriyama, M., 1999. Actual surface temperature measurement method using the thermoradiometer. In: Proc. 27th. Remote Sensing Society Japan conference, Remote Sens. Soc. J., pp. 85–86. (in Japanese).

[Moriyama, 2009] Moriyama, M., 2009. Investigation of the split window algorithm for the land surface tempe rature estimation. In: Proc. Fall Conf. of Japanese Photogrammeetry and Remote Sensing, pp. 65–68.

[Moriyama and Yano, 2000] Moriyama, M. and Yano, K., 2000. Time shift processing of the ground measured surface temperature for the satellite derived surface temperature validation. In: Proc. 29th. Remote Sensing Society Japan conference, Remote Sens. Soc. J., pp. 127–128. (in Japanese).

[Murayama and Moriyama, 1999] Murayama, T. and Moriyama, M., 1999. Development of the self–compensated thermoradiometer for the environmental temperature measurement. In: Proc. 27th. Remote Sensing Society Japan conference, Remote Sens. Soc. J., pp. 115–116. (in Japanese).

[Prata, 2002] Prata, F., 2002. Land surface temperature measurement from space: AATSR algorithm theoretical basis document. Technical report, CSIRO.

[Salisbery and D'Aria, 1985] Salisbery, J. W. and D'Aria, D. M., 1985. Emissivity of terrestrial materials in the 8 – 14 $\mu$m atmospheric window. Remote Sens. Environ. 42(2), pp. 83–106.

[Tayler, 1997] Tayler, J. R., 1997. An introduction to error analysis. University Science Books.

[Wan, 1999] Wan, Z., 1999. MODIS land–surface temperature algorithm theoretical basis document. Technical Report NAS5–31370, NASA.